15-Deoxy-$\Delta^{12,14}$-Prostaglandin J_2 Inhibits Transcriptional Activity of Estrogen Receptor-α via Covalent Modification of DNA-Binding Domain

Han-Jong Kim,[1] Joon-Young Kim,[1] Zhaojing Meng,[2] Li Hua Wang,[3] Fa Liu,[4] Thomas P. Conrads,[2] Terrence R. Burke,[4] Timothy D. Veenstra,[2] and William L. Farrar[1]

[1]Cancer Stem Cell Section, Laboratory of Cancer Prevention, [2]Laboratory of Proteomics and Analytical Technologies; and [3]Basic Research Program, Science Applications International Corporation-Frederick and [4]Laboratory of Medicinal Chemistry, Center for Cancer Research, National Cancer Institute, Frederick, Maryland

Abstract

The cyclopentenone 15-deoxy-$\Delta^{12,14}$-prostaglandin J_2 (15d-PGJ_2) inhibits proliferation of cancer cells, including breast cancers, by peroxisome proliferator-activated receptor-γ (PPARγ)–dependent and PPARγ-independent mechanisms. However, little is known about its effect on the transcriptional activity of estrogen receptor-α (ERα) that plays vital roles in the growth of breast cancers. Here, we show that 15d-PGJ_2 inhibits both 17β-estradiol (E_2)–dependent and E_2-independent ERα transcriptional activity by PPARγ-independent mechanism. In addition, 15d-PGJ_2 directly modifies ERα protein via its reactive cyclopentenone moiety, evidenced by incorporation of biotinylated 15d-PGJ_2 into ERα, both *in vitro* and *in vivo*. Nanoflow reverse-phase liquid chromatography tandem mass spectrometry analysis identifies two cysteines (Cys^{227} and Cys^{240}) within the COOH-terminal zinc finger of ERα DNA-binding domain (DBD) as targets for covalent modification by 15d-PGJ_2. Gel mobility shift and chromatin immunoprecipitation assays show that 15d-PGJ_2 inhibits DNA binding of ERα and subsequent repression of ERα target gene expression, such as *pS2* and *c-Myc*. Therefore, our results suggest that 15d-PGJ_2 can block ERα function by covalent modification of cysteine residues within the vulnerable COOH-terminal zinc finger of ERα DBD, resulting in fundamental inhibition of both hormone-dependent and hormone-independent ERα transcriptional activity. [Cancer Res 2007;67(6):2595–602]

Introduction

15-Deoxy-$\Delta^{12,14}$-prostaglandin J_2 (15d-PGJ_2), a cyclopentenone PG, is a naturally occurring derivative of PGD_2 and acts as an endogenous ligand for the nuclear receptor peroxisome proliferator-activated receptor-γ (PPARγ; refs. 1, 2). Growth-inhibitory effects of endogenous and synthetic PPARγ agonists have been shown in several tumors and cancer cell lines, including breast, colon, prostate, and lung cancers (3–8). The antitumorigenic effects of PPARγ agonists are caused by induction of cell cycle arrest, apoptosis, or differentiation through both PPARγ-dependent and PPARγ-independent mechanisms. They can induce cell cycle regulatory genes and inhibit genes involved in cell cycle progression or antiapoptotic proteins (8–11). In addition, 15d-PGJ_2 has been shown to interfere with the intracellular growth-promoting signaling through covalent modification of cysteines of target proteins such as IκB kinase, nuclear factor-κB (NF-κB), and activator protein-1 (AP-1), independently of PPARγ activation (12–14). J series of PGs, including 15d-PGJ_2, unlike other classes of PGs are characterized by the presence of a reactive α,β-unsaturated carbonyl group in the cyclopentenone ring. This moiety confers 15d-PGJ_2 the capability to form covalent adducts with thiols of cysteine residues in target proteins by Michael's addition, resulting in an alteration of protein function (12–15). Therefore, the growth inhibitory effect of 15d-PGJ_2 on tumor cells can be mediated in part by this highly reactive cyclopentenone moiety, independently of PPARγ activation.

Estrogen receptors (ERα and ERβ) are members of the steroid nuclear receptor superfamily that are hormone-regulated transcription factors and mediate the effects of estrogens and antiestrogens in breast cancers (16–19). ERα consists of several distinct functional domains: DNA-binding domain (DBD), ligand-binding domain (LBD), and transactivation domain. The NH_2-terminal domain of ERα contains a constitutive and ligand-independent transcriptional activation function (AF-1). The activity of AF-1 domain can be regulated by growth factors, such as insulin-like growth factor-I (IGF-1), epidermal growth factor (EGF), and transforming growth factor-α, via signal transduction cascades (20–24). The COOH-terminal LBD is a hydrophobic structure responsible for specific interactions with agonists and antagonists. The middle DBD contains two nonequivalent Cys^4 zinc fingers critical for binding to short palindromic nucleotide sequences called estrogen response element (ERE) in the target gene promoters. These two zinc fingers in ERα DBD function cooperatively in ERα dimerization and DNA binding (25, 26). In addition, the COOH-terminal zinc finger of ERα is structurally disordered, and the cysteine thiols of this zinc finger have been characterized as particularly susceptible to the attack of electrophilic agents such as 2,2′-dithiobisbenzamide-1 and benzisothiazolone (27–29).

Breast cancer is the most common cancer among western women, and ~70% of breast cancer patients are positive for ERα (30, 31). Current therapeutic strategy to treat ERα-positive breast cancer is based on the blockade of ERα transcriptional activity by selective ER modulators (SERM) such as tamoxifen. SERMs act as receptor-binding competitors of estrogens and block the effects of

Note: Supplementary data for this article are available at Cancer Research Online (http://cancerres.aacrjournals.org/).

The content of this publication does not necessarily reflect the views or policies of the Department of Health and Human Services, nor does mention of trade names, commercial products, or organizations imply endorsement by the U.S. government.

Requests for reprints: William L. Farrar, Laboratory of Cancer Prevention, National Cancer Institute-Frederick, Room 21–81, Building 560, 1050 Boyles Street, Frederick, MD 21702. Phone: 310-846-1503; Fax: 301-846-6019; E-mail: farrar@mail.ncifcrf.gov.

doi:10.1158/0008-5472.CAN-06-3043

estrogens. However, this antiestrogen therapy using tamoxifen is limited due to its partial estrogenic effects in endometrial cancers and resistance to its effects (20–22, 32). Moreover, crosstalk between ERα and growth factor signaling pathways, such as EGF and IGF-I, is postulated to be a critical factor especially in the mechanism of tamoxifen resistance in breast cancer (20–24).

In this study, we show that 15d-PGJ_2 inhibits 17β-estradiol (E_2)–dependent and E_2-independent ERα transcriptional activity by PPARγ-independent mechanism. We also show that 15d-PGJ_2 covalently modifies two cysteines in the vulnerable COOH-terminal zinc finger of ERα DBD and disrupts of the ERα zinc finger, resulting in inhibition of ERα DNA binding. In addition to defining the molecular mechanism underlying ERα inhibition by 15d-PGJ_2, our results validate targeting the vulnerable cysteines in the COOH-terminal zinc finger of ERα DBD by covalent modification or electrophilic attack as a means of disrupting hormone- and growth factor–mediated transactivation of ERα.

Materials and Methods

Chemicals and plasmids. 15d-PGJ_2 and 9,10-dihydro-15d-PGJ_2 (CAY10410) were obtained from Cayman Chemical (Ann Arbor, MI). GW9662, E_2, and rhIGF-I were obtained from Calbiochem (La Jolla, CA), Sigma-Aldrich (St. Louis, MO), and R&D Systems (Minneapolis, MN), respectively. The ERα and β-actin antibodies were obtained from Santa Cruz Biotechnology (Santa Cruz, CA). Formic acid and trifluoroacetic acid (TFA) were obtained from Fluka (Milwaukee, WI). High-performance liquid chromatography (HPLC)–grade acetonitrile was from EM Science (Darmstadt, Germany). ERE-tk-Luc, PPRE-tk-Luc, and expression vector for PPARγ (29) and ERβ expression plasmid (33) were described previously.

Cell culture and transient transfection assay. The human breast carcinoma cell lines MCF-7 ($ERα^+$, $ERβ^+$) and MDA-MB-231 ($ERα^-$, $ERβ^+$) were obtained from the American Type Culture Collection (Rockville, MD). MCF-7 and MDA-MB-231 cells were maintained with DMEM, supplemented with 10% fetal bovine serum (FBS) plus antibiotics. In experiments with E_2 and 15d-PGJ_2, cells were cultured in phenol red–free (PRF) DMEM supplemented with 0.5% charcoal-dextran–stripped FBS (CS-FBS; Hyclone, Logan, UT). Transient transfection assays were done using the FuGENE6 reagent (Roche Applied Science, Indianapolis, IN) according to the manufacturer's instructions. Cells ($4–8 \times 10^4$ per well) were split in 24-well plates the day before transfection in PRF DMEM supplemented with 10% CS-FBS. Twenty-four hours after transfection, medium was changed with PRF DMEM containing 0.5% CS-FBS. Cells were treated with DMSO (vehicle) or various concentrations of 15d-PGJ_2, CAY10410, or GW9662 together with or without E_2 for 5 h and harvested for luciferase and β-galactosidase assays. The luciferase activity was normalized by β-galactosidase activity.

Proliferation assay. Cell proliferation was examined by measuring DNA synthesis using tritiated thymidine (^{3}H-TdR) uptake. Cells were grown in PRF DMEM supplemented with 10% CS-FBS for 3 to 5 days. Quiescent cells (1×10^4 per well) were plated in triplicate in 96-well plates in 200 μL of growth media, containing 0.5% CS-FBS with or without E_2 together with DMSO or various concentration of 15d-PGJ_2 or CAY10410. After 68 h, cells were pulsed with [^{3}H]thymidine (0.5 μCi/100 μL) for 4 h, and [^{3}H]thymidine incorporation was analyzed by liquid scintillation counting.

Preparation of biotinylated 15d-PGJ_2. The carboxyl group of 15d-PGJ_2 was modified by amidation with EZ-link 5-(biotinamido)pentylamine (Pierce, Rockford, IL) by an alternate mixed anhydride procedure. Briefly, triethylamine and isobutyl chloroformate were added to a solution of 15d-PGJ_2 in anhydrous dichloromethane, and the reaction mixture was stirred at room temperature for 30 min. Solvent was removed *in vacuo*, and a solution of 5-(biotinamido)pentylamine in *N,N*-dimethylformamide was added followed by 4-dimethylaminopyridine in *N,N*-dimethylformamide, and the mixture was stirred overnight at room temperature. Biotinylated 15d-PGJ_2 was purified through a reverse-phase HPLC eluted using a VYDAC Protein and Peptide C_{18} column with a linear gradient of acetonitrile/water/acetic acid.

Labeling of ERα with biotinylated 15d-PGJ_2 *in vitro* and *in vivo*. For For *in vitro* labeling of ERα protein with biotinylated 15d-PGJ_2, purified ERα protein (Invitrogen, Carlsbad, CA) in 20 mmol/L Tris-HCl (pH 7), 45 mmol/L NaCl, 5 mmol/L $MgCl_2$, 0.1 mmol/L DTT, and 0.14% glycerol was incubated for 1 h at room temperature together with DMSO or biotinylated 15d-PGJ_2 in the presence or absence of excessive amount of 15d-PGJ_2 or CAY10410, or DTT. Incorporation of biotinylated 15d-PGJ_2 was assessed by Western blot with horseradish peroxidase–conjugated streptavidin (Pierce) and ECL (Pierce). ERα protein was detected in the reactions by Western blot using anti-ERα antibody. For *in vivo* incorporation of 15d-PGJ_2 into ERα in intact cells, MCF-7 cells were incubated with 10 μmol/L of biotinylated 15d-PGJ_2 for 2 h in PRF DMEM with 0.5% CS-FBS. Cells were lysed, and biotinylated proteins were purified by adsorption onto Neutravidin beads (Pierce). ERα and ERβ proteins were detected in the eluates by Western blot using anti-ERα and anti-ERβ antibodies.

Preparation of ERα peptides for mass spectrometric analysis. Purified ERα protein was incubated with DMSO or 15d-PGJ_2 (10 μmol/L) for 1 h at room temperature, lyophilized, and reconstituted in Laemmli gel loading buffer. The samples were resolved on a NuPAGE Bis-Tris gel (Invitrogen) and visualized by staining with SimplyBlue (Invitrogen). The protein bands were excised, destained, reduced, and alkylated before digestion with trypsin overnight at 37°C. Peptides were extracted and desalted using PepClean C-18 spin columns (Pierce) and resuspended in 0.1% TFA before mass spectrometry (MS) analysis.

Nanoflow reverse-phase liquid chromatography tandem MS. Nanoflow reverse-phase liquid chromatography tandem mass spectrometry (RPLC-MS/MS) was done using an Agilent 1100 nanoflow LC system (Agilent Technologies, Palo Alto, CA) coupled online with an linear ion-trap MS (LIT-MS; LTQ, ThermoElectron, San Jose, CA). Nanoflow RPLC columns were slurry-packed in-house with 5 μm, 300 Å pore size C-18 phase (Jupiter) in a 75 μm inner diameter × 10 cm fused silica capillary (Polymicro Technologies, Phoenix, AZ) with a flame pulled tip. After sample injection, the column was washed for 20 min with 98% mobile phase A (0.1% formic acid/water) at 0.5 μL/min, and peptides were eluted using a linear gradient of 2% to 42% mobile phase B (0.1% formic acid/acetonitrile) in 40 min at 0.25 μL/min, then to 98% mobile phase B in 10 min. The LIT-MS was operated in a data-dependent mode in which each full MS scan was followed by five MS/MS scans, where the five most abundant molecular ions were dynamically selected for collision-induced dissociation using normalized collision energy of 35%. Tandem mass spectra were searched using SEQUEST against a human proteome database and a mass difference of 57.0 Da (alkylation) or 316.4 Da (15d-PGJ_2 modification) was set as dynamic modification on cysteine residues in the search.

Zinc finger assay. Zinc finger assay was done as described (29). Time-dependent *in vitro* release of zinc from purified ERα protein treated with 15d-PGJ_2 or DMSO was measured using zinc-selective fluorescent probe *N*-(6-methoxy-8-quinolyl)-*p*-toluenesulfonamide (TSQ, Molecular Probes, Eugene, OR).

Gel mobility shift assay. The following end-labeled [^{32}P]oligonucleotide probes were used: ERE consensus sequence (Santa Cruz Biotechnology), 5′-GGATCTAGGTCACTGTGACCCCGGATC-3′. ERα protein was prepared by *in vitro* translation using a coupled transcription and translation system (TNT-coupled reticulocyte lysate system, Promega, Madison, WI). ERα protein (3 μL) or unprogrammed lysates were mixed with 10,000 cpm of labeled ERE probes in 20 μL of each reaction. After a 15-min incubation at room temperature, DNA protein complexes were analyzed on 5% polyacrylamide gel in 0.5 × Tris-borate EDTA (90 mmol/L Tris, 90 mmol/L boric acid, 2 mmol/L EDTA). Gels were dried and analyzed by autoradiography.

Chromatin immunoprecipitation assay. The chromatin immunoprecipitation assay was done as described previously (34). Briefly, MCF-7 cells were treated with 15d-PGJ_2 or DMSO in the presence of E_2. Cells were fixed with 1% formaldehyde and harvested. Soluble chromatin was immunoprecipitated with ERα or ERβ antibodies. The final DNA extractions were amplified by 30 cycles of PCR using primers from −519 to −220 bp region of the *pS2* gene promoter. The primers used for PCR are as follows:

pS2 (−519) forward, 5′-CGTGAGCCACTGCGCCAG-3′ and pS2 (−220) reverse, 5′-TCAGAAAGTCCCTCTTTC-3′. To quantitate relative binding of ERα or ERβ to *pS2* promoter, densitometric analysis was done using ImageQuant software (Amersham, Arlington Heights, IL). Band density was normalized to 10% input and presented as fold change relative to basal ERα or ERβ binding to *pS2* promoter in the absence of E_2.

Semiquantitative reverse transcription-PCR analysis. MCF-7 cells were treated with 15d-PGJ$_2$ or DMSO in the presence or absence of E_2 for 2 h. Cells were harvested for total RNA isolation using the TRIzol reagent (Invitrogen). First-strand cDNA was synthesized from 3 μg of total RNA using an oligo(dT) primers and reverse transcriptase. The resulting first-strand cDNA was then amplified to measure mRNA levels of pS2, c-Myc, and β-actin by 30, 30, and 25 cycles of PCR, respectively, using specific primers. The primer sequences used for PCR to detect pS2 and c-Myc mRNA are as follows: pS2 forward, 5′-ATGGCCACCATGGAGAACAAG-3′ and pS2 reverse, 5′-GGGACGGCACCGCGTCAGGAT-3′; c-Myc forward, 5′-GCAAGGACGC-GACTCTCCCGA-3′ and c-Myc reverse, 5′-CTCGAATTTCTTCCAGATATC-3; and β-actin forward, 5′-ATATCGCTGCGCTGGTCGTC-3′ and β-actin reverse, 5′-GATGGGCACAGTGTGGGTGA-3′. Band density was normalized to β-actin signals and presented as fold change relative to basal mRNA levels of pS2 or c-Myc.

Results

15d-PGJ$_2$ inhibits both E_2-dependent and E_2-independent ERα transcriptional activity. 15d-PGJ$_2$ has been shown to inhibit proliferation and induce apoptosis of breast cancer cells, and ~70% of breast cancer patients are positive for ERα (30, 31). To investigate the effect of 15d-PGJ$_2$ on the ERα transcriptional activity, MCF-7 (ERα$^+$, ERβ$^+$) and MDA-MB-231 (ERα$^-$, ERβ$^+$) cells were transiently transfected with ERE-driven luciferase construct. As shown in Fig. 1*A*, 15d-PGJ$_2$ dramatically reduced E_2-induced ERE luciferase activity in a dose-dependent manner only in ERα-positive MCF-7 cells. In contrast, 15d-PGJ$_2$ had little effect on ERβ-mediated transactivation in MDA-MB-231 cells transfected with ERβ expression vector (Fig. 1*B*), suggesting that ERα but not ERβ is a specific target for inhibition by 15d-PGJ$_2$. Notably, 15d-PGJ$_2$ strongly decreased basal luciferase activity of ERE in MCF-7 even in the absence of E_2. This observation raised the possibility that ligand-independent transactivity of ERα could also be repressed by 15d-PGJ$_2$. To address this hypothesis, we examined the effect of 15d-PGJ$_2$ on IGF-1–induced transactivation of ERα. As previously reported (35), IGF-1 increased ERE reporter activity possibly through activation of the AF-1 domain of ERα, and 15d-PGJ$_2$ visibly inhibited IGF-1–induced ERα transactivity (Fig. 1*C*). These findings suggest that 15d-PGJ$_2$ inhibits E_2-dependent and E_2-independent ERα transactivity.

Based on the inhibition of ERα transactivity by 15d-PGJ$_2$, to investigate the effect of 15d-PGJ$_2$ on ERα-mediated proliferation of breast cancer cells, [^{3}H]thymidine incorporation assay was done in MCF-7 and MDA-MB-231 cells. Cells were treated in the absence or presence of E_2 with 15d-PGJ$_2$ or 9,10-dihydro-15d-PGJ$_2$ (CAY10410),

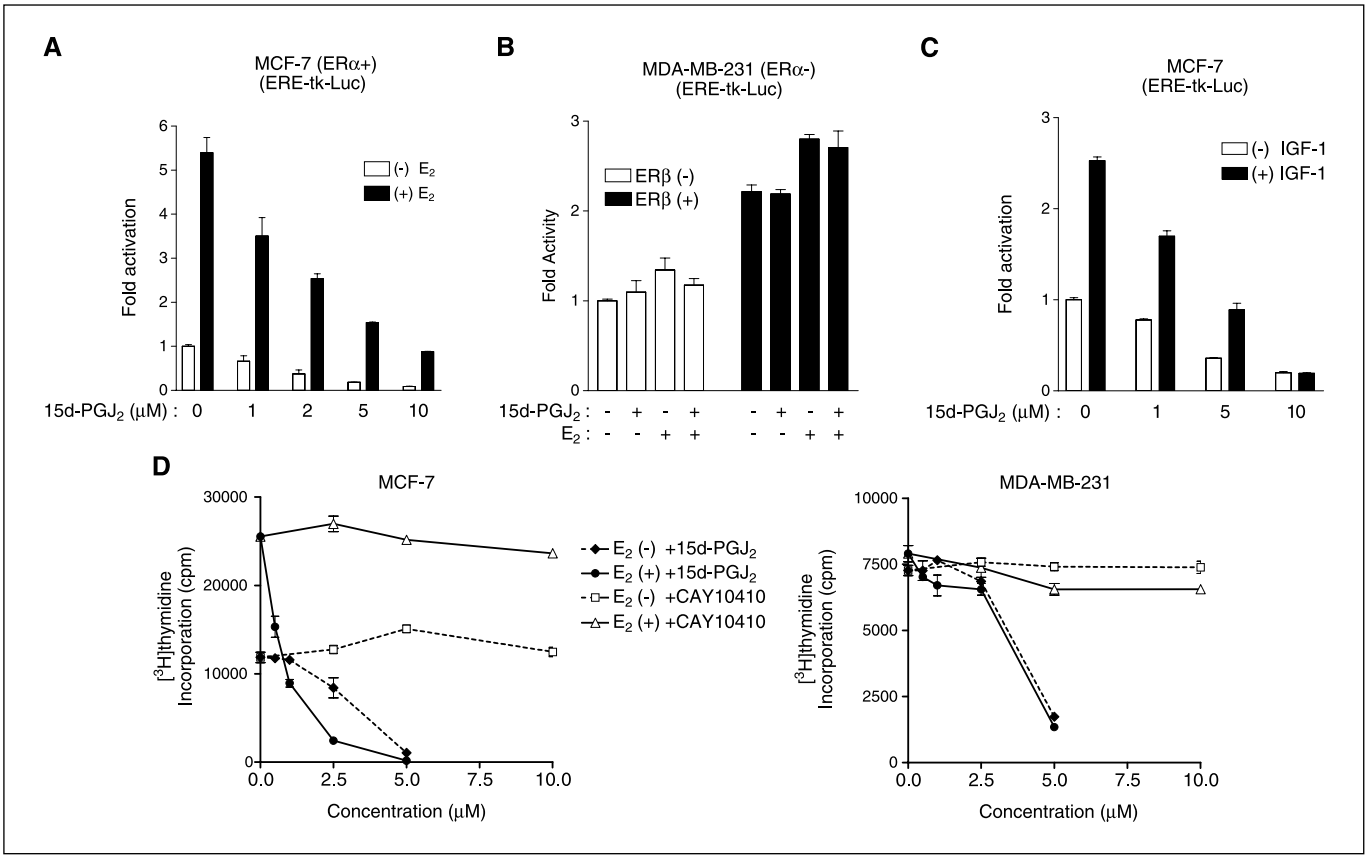

Figure 1. 15d-PGJ$_2$ inhibits E_2-dependent and E_2-independent ERα transcriptional activity. *A,* inhibition of basal and E_2-induced ERα transcriptional activity by 15d-PGJ$_2$ in MCF-7 (ERα$^+$) cells. *B,* 15d-PGJ$_2$ (10 μmol/L) had little effect on either basal or ERβ-mediated transactivation of ERE-tk-Luc in MDA-MB-231 (ERα$^-$) cells. *C,* effect of 15d-PGJ$_2$ on IGF-1–dependent ERα transactivity in MCF-7 cells. MCF-7 (*A* and *C*) and MDA-MB-231 (*B*) cells were transiently transfected with ERE-tk-Luc together with expression vector for ERβ (*B*) and treated with various concentrations of 15d-PGJ$_2$ with or without E_2 (100 nmol/L) or IGF-1 (50 ng/mL). After 5 h of treatment, cells were lysed and assayed for luciferase activity. *D,* effect of 15d-PGJ$_2$ on proliferation of MCF-7 and MDA-MB-231 cells. Cells were treated with various concentrations of 15d-PGJ$_2$, CAY10410, or DMSO (vehicle) with or without E_2 (5 nmol/L) for 72 h as indicated. Cell proliferation was examined by DNA synthesis using [^{3}H]thymidine incorporation.

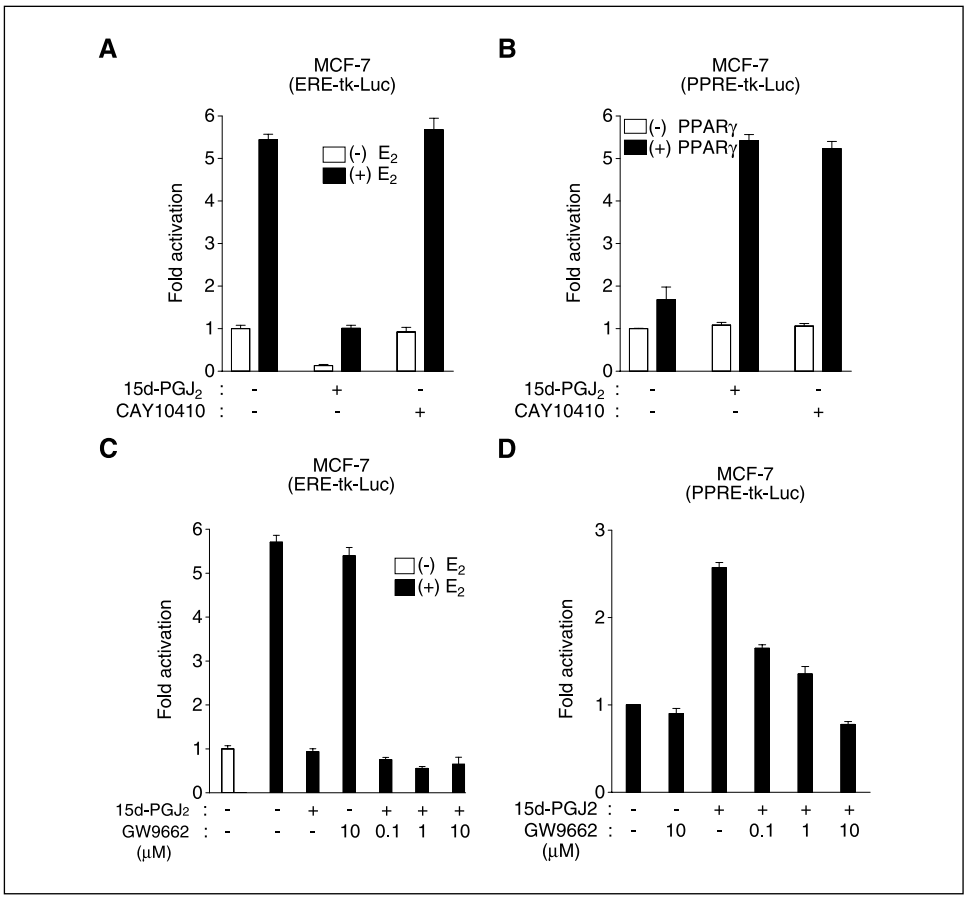

Figure 2. Inhibition of ERα transcriptional activity by 15d-PGJ_2 through PPARγ-independent mechanism. *A,* transactivity of ERα is inhibited by 15d-PGJ_2 but not by the synthetic PPARγ ligand CAY10410. *B,* PPARγ-dependent transactivation is stimulated by both 15d-PGJ_2 and CAY10410. *C,* GW9662, a selective PPARγ antagonist, does not reverse 15d-PGJ_2–induced repression of ERα transcriptional activity, whereas it strongly reverses the 15d-PGJ_2–induced activation of PPARγ-dependent transactivation (*D*). MCF-7 cells were transfected with ERE-tk-Luc (*A* and *C*) and PPRE-tk-Luc together with expression vector for PPARγ (*B* and *D*). After 24 h, cells were treated for 5 h with 10 μmol/L 15d-PGJ_2 or CAY10410 and indicated concentration of GW9662 together with or without E_2 (100 nmol/L) as indicated.

a natural or a synthetic agonist of PPARγ, respectively. As shown in Fig. 1*D*, E_2 significantly stimulated [^{3}H]thymidine incorporation in MCF-7 cells but not in MDA-MB-231 cells. 15d-PGJ_2 at low concentration (0.5–2.5 μmol/L) drastically decreased the proliferation of MCF-7 cells but not that of MDA-MB-231 cells. This inhibitory effect of 15d-PGJ_2 was much stronger in the presence of E_2 possibly due to repression of ERα-mediated signaling pathway. Furthermore, 15d-PGJ_2 at higher concentration (5 μmol/L) greatly blocked proliferation of both MCF-7 and MDA-MB231 cells, irrespective of the presence of E_2 possibly due to induction of apoptosis, suggesting ERα-independent mechanism. In contrast, CAY10410 had little effect on proliferation of either cells even at the higher concentration (10 μmol/L), suggesting that PPARγ activation may not be required for the inhibitory effect of 15d-PGJ_2. Taken together, these results show that 15d-PGJ_2 inhibits E_2-dependent and E_2-independent ERα transactivity and subsequent ERα-mediated proliferation of breast cancer cells.

15d-PGJ_2 inhibits ERα transcriptional activity through PPARγ-independent mechanism. To further assess the requirement of PPARγ for ERα inhibition by 15d-PGJ_2, MCF-7 cells were treated with CAY10410 and GW9662, a synthetic agonist and an antagonist for PPARγ, respectively. As shown in Fig. 2*A*, CAY10410 did not have any effect on ERα transactivity, whereas it had similar potency comparable to that of 15d-PGJ_2, to activate PPRE luciferase reporter that contains PPARγ response elements (Fig. 2*B*). Moreover, GW9662, a selective PPARγ antagonist did not reverse the repression of ERα by 15d-PGJ_2, whereas it completely blocked 15d-PGJ_2–induced PPRE-driven luciferase activity (Fig. 2*C* and *D*). A similar result was obtained in PPARγ-negative HeLa cells (9, 36) transiently transfected with ERα expression vector and ERE luciferase reporter (data not shown). These results reveal that 15d-PGJ_2 inhibits ERα transactivity through PPARγ-independent mechanism.

Direct modification of ERα protein by 15d-PGJ_2. It has been shown that 15d-PGJ_2 covalently modifies cysteines in several cellular proteins and alter their function (12–15, 36, 37). The cyclopentenone moiety of 15d-PGJ_2 has the capacity to directly react with sulfhydryl group of cysteine residues of the proteins by Michael's addition. The only structural difference of CAY10410 from 15d-PGJ_2 is its lack of cyclopentenone moiety (Fig. 3*A*). To examine whether 15d-PGJ_2 can directly modify ERα protein via its cyclopentenone moiety independently of PPARγ, we synthesized biotinylated 15d-PGJ_2 and examined its direct interaction with purified ERα protein. As shown in Fig. 3*B*, biotinylated 15d-PGJ_2 directly incorporated into ERα protein under the *in vitro* condition. This incorporation was completely blocked by excessive amount of unlabeled 15d-PGJ_2 but not CAY10410 (Fig. 3*C*), showing the specificity and the involvement of cyclopentenone moiety of 15d-PGJ_2 in the modification of ERα. In addition, this ERα modification by biotinylated 15d-PGJ_2 was significantly diminished in the presence of 10 mmol/L DTT, suggesting the involvement of modification of thiol groups in cysteine residues of ERα (Fig. 3*C*).

To explore the *in vivo* modification, MCF-7 cells were treated with biotinylated 15d-PGJ_2 or DMSO, and whole-cell lysates were probed with streptavidin. An estimated ERα band was identifiable among several target proteins only in the cell lysates treated with

15d-PGJ$_2$ but not DMSO (Supplementary Fig. S1). To further verify *in vivo* modification of ERα by 15d-PGJ$_2$, cell lysates were subjected to pull-down assay using Neutravidin beads and followed by Western blot with anti-ERα or anti-ERβ antibody. As shown in Fig. 3*D*, incorporation of biotinylated 15d-PGJ$_2$ into ERα *in vivo* was detected in the cells lysates treated with biotinylated 15d-PGJ$_2$ but not DMSO, whereas ERβ was not detected in either cell lysates, suggesting specific modification of ERα by 15d-PGJ$_2$. These results suggest that 15d-PGJ$_2$ may directly modify cysteines of ERα both *in vitro* and *in vivo* via its cyclopentenone moiety.

Identification of Cys^{277} and Cys^{240} within the COOH-terminal zinc finger of ERα DBD as targets for covalent modification by 15d-PGJ$_2$. To determine target cysteine residues in ERα for modification by 15d-PGJ$_2$, purified ERα protein was treated with 15d-PGJ$_2$ or DMSO followed by digestion with trypsin and analyzed by Nanoflow RPLC-MS/MS. The peptide sequences were identified by searching the tandem mass spectra against a human database with dynamic modifications on cysteine residues including 15d-PGJ$_2$ modification (316.4 Da). Among a total of 13 cysteines in ERα, 10 were not modified in the reaction condition (data not shown), and the Cys^{381}-containing peptide was not detected in either the control or the 15d-PGJ$_2$–treated sample; thus, the possibility of modification of Cys^{381} cannot be excluded. As shown in Fig. 4*A* and *B*, two peptides containing cysteines modified by 15d-PGJ$_2$ were detected. The tandem mass spectrum of a triply charged precursor ion at *m/z* 877.2 of the ERα peptide SIQGHNDYMC^{221}PATNQC^{227}TIDK is shown in Fig. 4*A*. The singly (b_2-b_{14}) and doubly (b_{14}, b_{14}-NH_3, and b_{15}-NH_3) charged NH_2-terminal product ions and the singly charged COOH-terminal fragment ion (y_2) were observed. The singly ($^*y_6$ and $^*y_{10}$) and doubly ($^*y_6^{+2}$) charged COOH-terminal fragment ions were observed to increase 316.4 Da. These observations reveal that the 15d-PGJ$_2$ covalently modifies Cys^{227} but not Cys^{221}. Figure 4*B* shows the tandem mass spectrum of the doubly charged ion at *m/z* 521.0 of 15d-PGJ$_2$–modified peptide SC^{237}QAC^{240}R. The singly charged NH_2-terminal fragments (b_2-b_5) and COOH-terminal fragment (y_1) were observed. In addition, the singly charged NH_2-terminal fragment ($^*b_5$) and the singly ($^*y_2$-$^*y_5$) and doubly ($^*y_5^{+2}$) charged COOH-terminal fragments were observed to increase 316.4 Da, suggesting that Cys^{240} but not Cys^{237} is the target for 15d-PGJ$_2$ modification. Consistent with the previous studies (27–29), these results show that 15d-PGJ$_2$ modifies two cysteines (Cys^{227} and Cys^{240}) located in the COOH-terminal zinc finger of ERα DBD that is structurally disordered and susceptible to electrophilic attack (Fig. 4*C*).

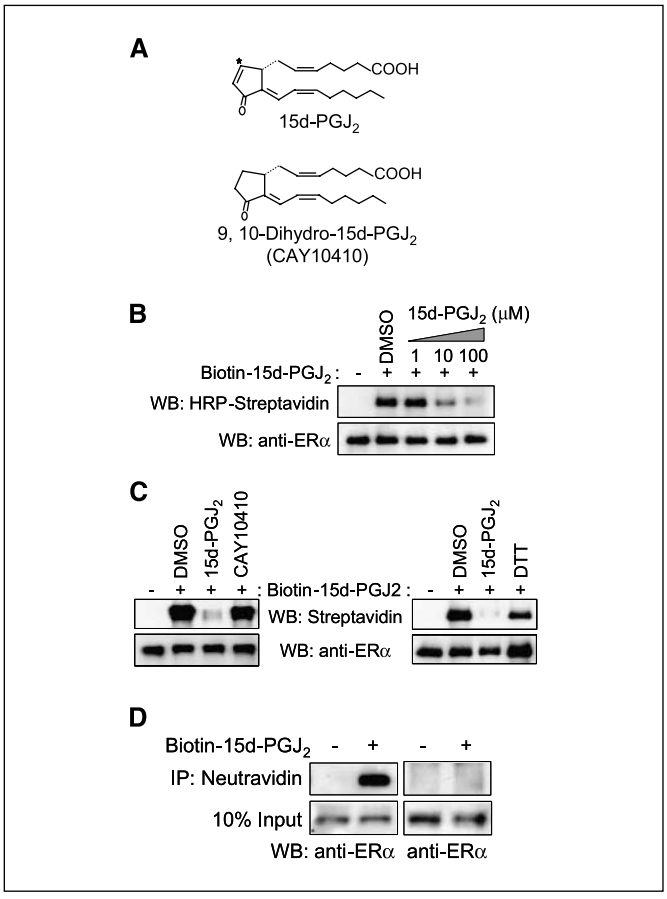

Figure 3. 15d-PGJ$_2$ directly binds to ERα *in vitro* and *in vivo*. *A,* structures of 15d-PGJ$_2$ and CAY10410. *, reactive α,β-unsaturated carbonyl group. *B* and *C, in vitro* labeling of ERα with 15d-PGJ$_2$. Purified human ERα protein (100 ng) was incubated with biotinylated 15d-PGJ$_2$ (1 μmol/L) in the absence or presence of 15d-PGJ$_2$ (100 μmol/L), CAY10410 (100 μmol/L), or DTT (10 mmol/L) at room temperature for 1 h as indicated. Incubation mixtures were subjected to SDS-PAGE and Western blot (*WB*) with horseradish peroxidase (*HRP*)–conjugated streptavidin or anti-ERα antibody. *D,* incorporation of 15d-PGJ$_2$ into ERα but not ERβ *in vivo*. MCF-7 cells were treated with biotinylated 15d-PGJ$_2$ (10 μmol/L) for 2 h. Cell lysates were subjected to pull-down assay with Neutravidin beads. Incorporation of biotinylated 15d-PGJ$_2$ into endogenous ERα and 10% of total lysates used for the reaction as input were assessed by Western blot with anti-ERα or ERβ antibody as indicated. *IP,* immunoprecipitation.

Based on the observation that 15d-PGJ$_2$ modifies two cysteines in the COOH-terminal zinc finger of ERα DBD, the effect of 15d-PGJ$_2$ on the zinc finger function of ERα was investigated by performing *in vitro* zinc finger assay. As shown in Fig. 4*D*, zinc was released from recombinant ERα protein treated with 15d-PGJ$_2$ but not with DMSO control in a time-dependent manner, showing that 15d-PGJ$_2$ disrupts the zinc finger of ERα DBD. Taken together, these results suggest that 15d-PGJ$_2$ covalently modifies two cysteines in the COOH-terminal zinc finger of ERα DBD, resulting in disruption of zinc finger function of ERα.

Inhibition of DNA binding of ERα by 15d-PGJ$_2$. The COOH-terminal zinc finger of ERα is structurally disordered and labile; thus, cysteine thiols in this zinc finger are more susceptible to electrophilic attack, resulting in loss of ERα dimerization and DNA binding function (27–29). In good agreement with these reports, our results showed 15d-PGJ$_2$ disrupts ERα zinc finger function by covalent modification of cysteines in the vulnerable COOH-terminal zinc finger of ERα DBD. Based on these observations, the possibility that 15d-PGJ$_2$ can alter the DNA binding function of ERα was investigated by gel mobility shift assay. As shown in Fig. 5*A*, *in vitro* translated ERα protein bound to ^{32}P-labeled ERE probes, as shown by ERα-specific antibody supershift. The formation of ERα-ERE complex was exclusively blocked by 15d-PGJ$_2$ but not by CAY10410 (Fig. 5*B*). This result shows that 15d-PGJ$_2$ directly inhibits DNA binding of ERα through covalent modification of cysteines in the zinc finger of ERα DBD and disruption of zinc finger function of ERα.

To further confirm the inhibition of DNA binding of ERα by 15d-PGJ$_2$ *in vivo*, chromatin immunoprecipitation assay was carried out using ERα or ERβ antibody after treatment of 15d-PGJ$_2$ in MCF-7 cells. As shown in Fig. 5*C*, densitometric analysis revealed that E_2 enhanced up to 7-fold ERα binding to the *pS2* gene promoter that contains an ER-binding site, whereas E_2 had little effect on ERβ binding to the promoter. Consistent with the result from gel

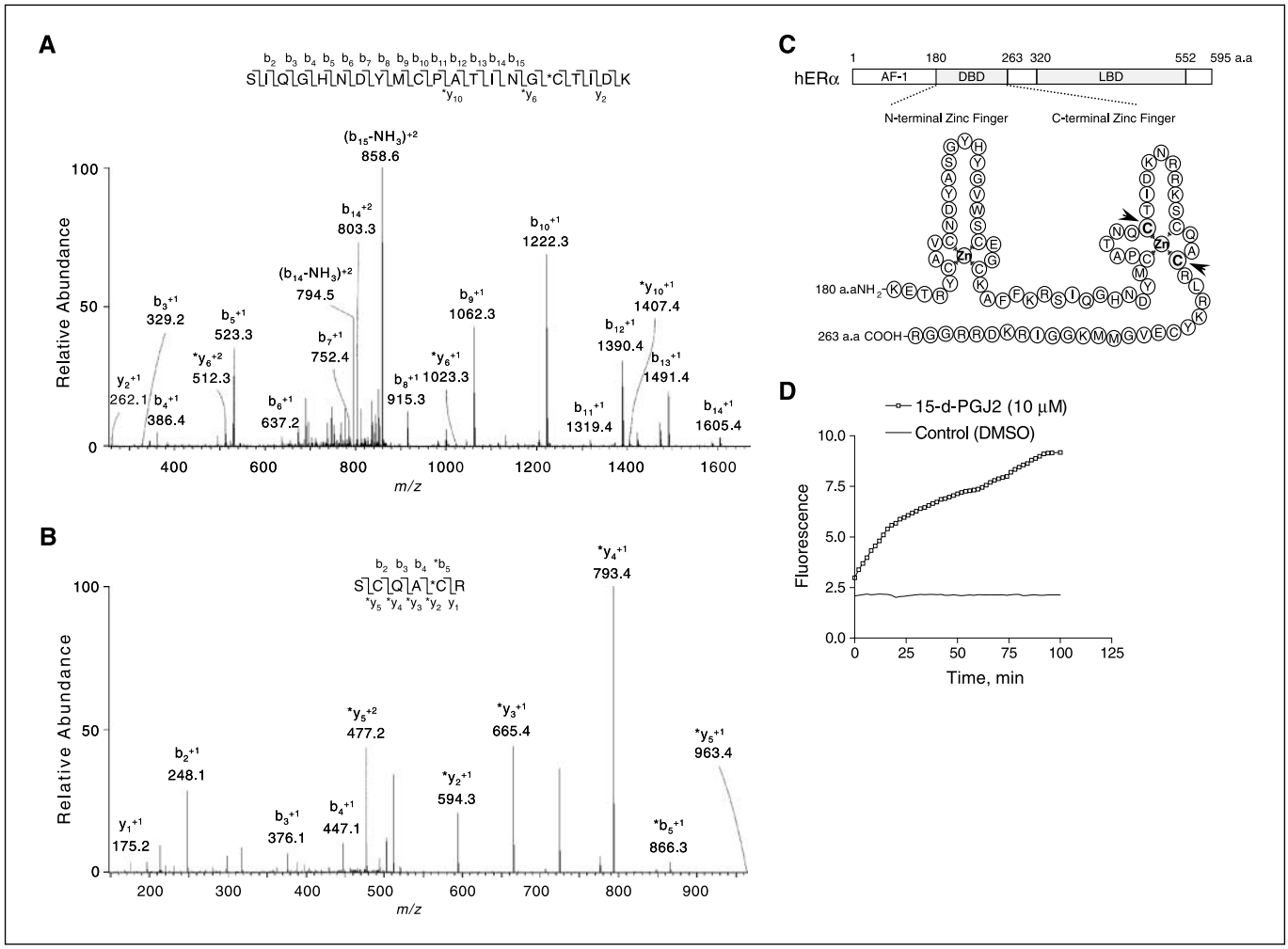

Figure 4. Cys^{227} and Cys^{240} within the COOH-terminal zinc finger of ERα DBD are identified as targets for covalent modification by 15d-PGJ_2. *A* and *B,* tandem mass spectra of the 15d-PGJ_2–modified ERα peptides SIQGHNDYMC^{221}PATING*C^{227}TIDK (*A*) and SC^{237}QA*C^{240}R (*B*). *C, 15d-PGJ_2–modified cysteine residues. *C,* schematic representation of two zinc fingers of ERα DBD (180–263 amino acids). *Arrowheaded Cs in bold,* Cys^{227} and Cys^{240} within the COOH-terminal zinc finger of ERα DBD modified by 15d-PGJ_2. *D,* disruption of ERα zinc finger function by 15d-PGJ_2. Time-dependent release of zinc ion from the purified ERα protein treated with 15d-PGJ_2 or DMSO was measured by zinc finger assay using zinc selective fluorescent probe (TSQ).

mobility shift assay, E_2-enhanced binding of ERα to the *pS2* promoter was completely abrogated by 15d-PGJ_2 but not by CAY10410. In contrast, 15d-PGJ_2 had little effect on ERβ binding to *pS2* promoter, supported by the results from transient transfection assay (Fig. 1*B*) and *in vivo* labeling of ER proteins by biotin-15d-PGJ_2 (Fig. 3*D*). Consistent with the results from chromatin immunoprecipitation assay, 15d-PGJ_2 notably reduced both basal and E_2-enhanced mRNA levels of *pS2* and *c-Myc*, which are well-characterized ERα target genes (38), as verified by semiquantitative reverse transcription-PCR (Fig. 5*D*). This finding indicates that 15d-PGJ_2 represses the transcription of ERα target genes *pS2* and *c-Myc* by inhibition of ERα binding to target gene promoters. Taken together, these results suggest that 15d-PGJ_2 suppresses ERα-mediated transcription by inhibition of ERα DNA binding function.

Discussion

PPARγ agonists, including 15d-PGJ_2, have been shown to inhibit proliferation of breast cancer cells (4, 5, 9, 10, 39). Our result shows that 15d-PGJ_2 at low concentration (0.5–2.5 μmol/L) strongly decreases proliferation of ERα-positive MCF-7 cells in the absence or presence of E_2 but not that of ERα-negative MDA-MB-231 cells (Fig. 1*D*). This observation proposes that inhibitory effect of 15d-PGJ_2 on the proliferation of MCF-7 cells can be in part due to the repression of ERα-mediated signaling pathway. In addition, 15d-PGJ_2 potently suppresses the proliferation of MDA-MB-231 cells as well as MCF-7 cells at high concentration (≥5 μmol/L). Constitutive activation of NF-κB and AP-1 has been linked to the development of hormone-independent, ERα-negative human breast cancer cells such as MDA-MB-231 cells (29, 40). Therefore, it is assumed that 15d-PGJ_2 at high concentration can inhibit cell proliferation of MDA-MB-231 cells possibly by affecting multiple signaling pathways, including NF-κB and AP-1, as well as unknown targets, independently of ERα.

Previous study has shown that 15d-PGJ_2 and a synthetic PPARγ ligand (ciglitazone) induce proteasome-dependent degradation of cyclin D1 and ERα, in a PPARγ-dependent manner, resulting in PPARγ-mediated growth arrest in breast cancer cells (39). We also observed that ERα protein was ubiquitinated after treatment of 15d-PGJ_2 (Supplementary Fig. S2) as previously reported (39).

However, our results also showed that 15d-PGJ$_2$ inhibits ERα transactivity through blocking of ERα DNA binding via direct modification of ERα, independently of PPARγ. Therefore, these findings suggest that 15d-PGJ$_2$–adducted ERα, which is not able to bind to and transactivate the target gene promoters, should be a target for proteasome-dependent degradation through PPARγ-dependent mechanism.

Growth factors, including IGF-1, have been shown to stimulate proliferation of breast cancer cells through crosstalk with ERα (20–24). Phosphorylation of the AF-1 domain of ERα by mitogen-activated protein kinase or AKT, which are downstream signaling molecules activated by growth factors, plays important roles in E$_2$-independent ERα transactivation and growth of ERα-positive breast cancer cells. The activated AF-1 domain of ERα can recruit coactivators, such as amplified in breast cancer 1 or SRC-1, even in the presence of antiestrogens such as tamoxifen. This is considered as one of the mechanisms of resistance to antiestrogen therapy. In addition to antiestrogen, therapy using aromatase inhibitors aims also to obstruct ERα transactivity by deprivation of ER ligand E$_2$.

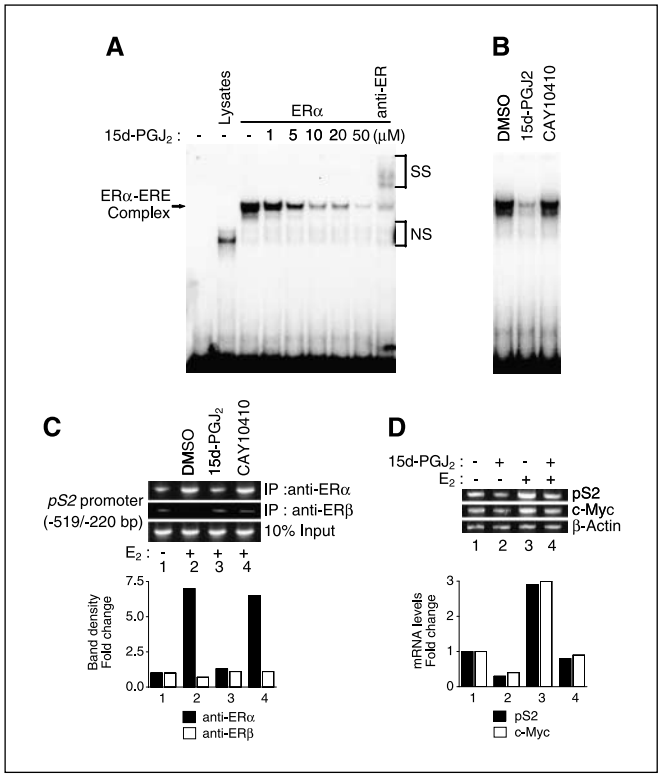

Figure 5. 15d-PGJ$_2$ directly inhibits the DNA-binding activity of ERα. *A* and *B,* gel mobility shift assay. DNA binding of ERα is inhibited by 15d-PGJ$_2$ but not by CAY10410 (*B*). ^{32}P-labeled ERE probes were incubated with *in vitro* translated ERα (3 μL) protein or unprogrammed lysates. Anti-ERα antibody was used for supershift (*SS*). *NS,* nonspecific. *C,* chromatin immunoprecipitation assay. MCF-7 cells were treated with 10 μmol/L 15d-PGJ$_2$ or CAY10410 in the presence of E$_2$ (100 nmol/L) for 2 h. Soluble chromatin from these cells was prepared and immunoprecipitated with an ERα- or ERβ-specific antibody. The PCR fragment from −519 to −220 bp (300 bp) on the *pS2* gene promoter contains an ERE, and 10% of the soluble chromatin used in the reaction was used as inputs. *D,* semiquantitative reverse transcription-PCR analysis. mRNA expression levels of ERα target genes *pS2* and *c-Myc* were reduced by 15d-PGJ$_2$. MCF-7 cells were incubated with 15d-PGJ$_2$ (10 μmol/L) in the presence or absence of E$_2$ (100 nmol/L) for 6 h. Total RNA was isolated from cells and analyzed by reverse transcription-PCR. *C* and *D, bottom,* graphic presentation of densitometric analyses of chromatin immunoprecipitation and semiquantitative reverse transcription-PCR.

However, these therapeutic approaches have limitation due to the fact that ERα still binds to its target gene promoters and mediates growth-promoting signaling by growth factors or partial estrogenic antiestrogens. Our results showed that 15d-PGJ$_2$ represses both basal and IGF-1–induced ERα transcriptional activity as well as E$_2$-dependent ERα activation (Fig. 1*A* and *C*). In addition, 15d-PGJ$_2$ directly blocks the DNA binding of ERα to ERE *in vitro* and to its binding sites on the target gene promoters *in vivo* (Fig. 5) through disruption of zinc finger function of ERα DBD (Fig. 4). Thus, our findings suggest that 15d-PGJ$_2$ can block the ERα-mediated transcription induced by growth factors and antiestrogens as well as E$_2$, resulting in growth inhibition of ERα-positive breast cancer cells. This is very important because DNA binding inhibition of ERα can be a more fundamental approach to block the ERα transcriptional activity than antagonism or deprivation of E$_2$. Because the physiologic concentration of 15d-PGJ$_2$ is in the picomolar to nanomolar range (41, 42), the micromolar concentrations of 15d-PGJ$_2$ typically used in our and other studies may not be physiologically relevant. However, our study provides a new approach for development of drugs derived from 15d-PGJ$_2$ that contains the reactive cyclopentenone moiety to treat ERα-positive breast cancers.

The ERα DBD contains two functionally and structurally nonequivalent Cys[4] zinc finger motifs that are crucial to ERα-mediated transcription. The COOH-terminal zinc finger of ERα DBD is structurally disordered and susceptible to electrophilic attack as a monomer but is stabilized by dimerization (27–29). Our previous study showed that electrophilic agents, such as 2,2′-dithiobisbenzamide-1 and benzisothiazolone, preferentially disrupt the vulnerable COOH-terminal zinc finger of ERα DBD, resulting in inhibition of dimerization and DNA binding of ERα (29). In the present study, we identified Cys^{227} and Cys^{240} within the COOH-terminal zinc finger of ERα DBD as targets for covalent modification by 15d-PGJ$_2$ (Fig. 4). In addition, our zinc ejection experiment showed that 15d-PGJ$_2$ disrupts zinc finger function of ERα (Fig. 4), resulting in inhibition of ERα DNA binding and thus suppression of target gene transcription, such as the proto-oncogene *c-Myc* (Fig. 5). Therefore, the growth-inhibitory effect of 15d-PGJ$_2$ on ERα-positive breast cancers can be mediated by direct modification and disruption of zinc finger function of ERα DBD.

In summary, we have identified 15d-PGJ$_2$ as a potent inhibitor of ERα transactivity through direct covalent modification of ERα, independently of PPARγ. 15d-PGJ$_2$ directly adducts with Cys^{227} and Cys^{240} within the COOH-terminal zinc finger of ERα DBD, resulting in inhibition of both hormone-dependent and hormone-independent ERα-mediated transcription and growth in breast cancer cells. Therefore, our finding presents a novel approach to the design of new drugs to treat ERα-positive breast cancers based on covalent modification of cysteines within the vulnerable COOH-terminal zinc finger of ERα DBD and subsequent DNA binding inhibition of ERα rather than conventional antagonism of estrogen.

Acknowledgments

Received 8/16/2006; revised 12/14/2006; accepted 1/10/2007.

Grant support: Intramural Research Program of the National Cancer Institute, NIH and Federal funds from the National Cancer Institute, NIH under contract N01-CO-12400 (H-J. Kim, J-Y. Kim, and W.L. Farrar).

The costs of publication of this article were defrayed in part by the payment of page charges. This article must therefore be hereby marked *advertisement* in accordance with 18 U.S.C. Section 1734 solely to indicate this fact.

References

1. Forman BM, Tontonoz P, Chen J, Brun RP, Spiegelman BM, Evans RM. 15-Deoxy-$\Delta^{12,14}$-prostaglandin J_2 is a ligand for the adipocyte determination factor PPARγ. Cell 1995;83:803–12.
2. Kliewer SA, Lenhard JM, Willson TM, Patel I, Morris DC, Lehmann JM. A prostaglandin J_2 metabolite binds peroxisome proliferator-activated receptor γ and promotes adipocyte differentiation. Cell 1995;83:813–9.
3. Lehrke M, Lazar MA. The many faces of PPARγ. Cell 2005;123:993–9.
4. Grommes C, Landreth GE, Heneka MT. Antineoplastic effects of peroxisome proliferator-activated receptor γ agonists. Lancet Oncol 2004;5:419–29.
5. Clay CE, Atsumi GI, High KP, Chilton FH. Early *de novo* gene expression is required for 15-deoxy-$\Delta^{12,14}$-prostaglandin J_2-induced apoptosis in breast cancer cells. J Biol Chem 2001;276:47131–5.
6. Sarraf P, Mueller E, Jones D, et al. Differentiation and reversal of malignant changes in colon cancer through PPARγ. Nat Med 1998;4:1046–52.
7. Chaffer CL, Thomas DM, Thompson EW, Williams ED. PPARγ-independent induction of growth arrest and apoptosis in prostate and bladder carcinoma. BMC Cancer 2006;6:53.
8. Han S, Sidell N, Fisher PB, Roman J. Up-regulation of p21 gene expression by peroxisome proliferator-activated receptor γ in human lung carcinoma cells. Clin Cancer Res 2004;10:1911–9.
9. Patel L, Pass I, Coxon P, Downes CP, Smith SA, Macphee CH. Tumor suppressor and anti-inflammatory actions of PPARγ agonists are mediated via upregulation of PTEN. Curr Biol 2001;11:764–8.
10. Wang C, Fu M, D'Amico M, et al. Inhibition of cellular proliferation through IκB kinase-independent and peroxisome proliferator-activated receptor γ-dependent repression of cyclin D1. Mol Cell Biol 2001;21:3057–70.
11. Chen GG, Lee JF, Wang SH, Chan UP, Ip PC, Lau WY. Apoptosis induced by activation of peroxisome-proliferator activated receptor-γ is associated with Bcl-2 and NF-κB in human colon cancer. Life Sci 2002;70:2631–46.
12. Rossi A, Kapahi P, Natoli G, et al. Anti-inflammatory cyclopentenone prostaglandins are direct inhibitors of IκB kinase. Nature 2000;403:103–8.
13. Cernuda-Morollon E, Pineda-Molina E, Canada FJ, Perez-Sala D. 15-Deoxy-$\Delta^{12,14}$-prostaglandin J_2 inhibition of NF-κB-DNA binding through covalent modification of the p50 subunit. J Biol Chem 2001;276:35530–6.
14. Perez-Sala D, Cernuda-Morollon E, Canada FJ. Molecular basis for the direct inhibition of AP-1 DNA binding by 15-deoxy-$\Delta^{12,14}$-prostaglandin J_2. J Biol Chem 2003;278:51251–60.
15. Shibata T, Yamada T, Ishii T, et al. Thioredoxin as a molecular target of cyclopentenone prostaglandins. J Biol Chem 2003;278:26046–54.
16. Mangelsdorf DJ, Thummel C, Beato M, et al. The nuclear receptor superfamily: the second decade. Cell 1995;83:835–9.
17. Tsai MJ, O'Malley BW. Molecular mechanisms of action of steroid/thyroid receptor superfamily members. Annu Rev Biochem 1994;63:451–86.
18. Hall JM, Couse JF, Korach KS. The multifaceted mechanisms of estradiol and estrogen receptor signaling. J Biol Chem 2001;276:36869–72.
19. Shang Y, Brown M. Molecular determinants for the tissue specificity of SERMs. Science 2002;295:2465–8.
20. Lewis JS, Jordan VC. Selective estrogen receptor modulators (SERMs): mechanisms of anticarcinogenesis and drug resistance. Mutat Res 2005;591:247–63.
21. Gururaj AE, Rayala SK, Vadlamudi RK, Kumar R. Novel mechanisms of resistance to endocrine therapy: genomic and nongenomic considerations. Clin Cancer Res 2006;12:1001–7s.
22. Schiff R, Massarweh SA, Shou J, Bharwani L, Mohsin SK, Osborne CK. Cross-talk between estrogen receptor and growth factor pathways as a molecular target for overcoming endocrine resistance. Clin Cancer Res 2004;10:331–6S.
23. Font de Mora J, Brown M. AIB1 is a conduit for kinase-mediated growth factor signaling to the estrogen receptor. Mol Cell Biol 2000;20:5041–7.
24. Kato S, Endoh H, Masuhiro Y, et al. Activation of the estrogen receptor through phosphorylation by mitogen-activated protein kinase. Science 1995;270:1491–4.
25. Schwabe JW, Chapman L, Finch JT, Rhodes D. The crystal structure of the estrogen receptor DNA-binding domain bound to DNA: how receptors discriminate between their response elements. Cell 1993;75:567–78.
26. Schwabe JW, Neuhaus D, Rhodes D. Solution structure of the DNA-binding domain of the oestrogen receptor. Nature 1990;348:458–61.
27. Maynard AT, Covell DG. Reactivity of zinc finger cores: analysis of protein packing and electrostatic screening. J Am Chem Soc 2001;123:1047–58.
28. Whittal RM, Benz CC, Scott G, Semyonov J, Burlingame AL, Baldwin MA. Preferential oxidation of zinc finger 2 in estrogen receptor DNA-binding domain prevents dimerization and, hence, DNA binding. Biochemistry 2000;39:8406–17.
29. Wang LH, Yang XY, Zhang X, et al. Suppression of breast cancer by chemical modulation of vulnerable zinc fingers in estrogen receptor. Nat Med 2004;10:40–7.
30. Leclercq G, Lacroix M, Laios I, Laurent G. Estrogen receptor α: impact of ligands on intracellular shuttling and turnover rate in breast cancer cells. Curr Cancer Drug Targets 2006;6:39–64.
31. Ariazi EA, Ariazi JL, Cordera F, Jordan VC. Estrogen receptors as therapeutic targets in breast cancer. Curr Top Med Chem 2006;6:181–202.
32. Shang Y. Molecular mechanisms of oestrogen and SERMs in endometrial carcinogenesis. Nat Rev Cancer 2006;6:360–8.
33. Monroe DG, Johnsen SA, Subramaniam M, et al. Mutual antagonism of estrogen receptors α and β and their preferred interactions with steroid receptor coactivators in human osteoblastic cell lines. J Endocrinol 2003;176:349–37.
34. Kim HJ, Kim JY, Kim JY, et al. Differential regulation of human and mouse orphan nuclear receptor small heterodimer partner promoter by sterol regulatory element binding protein-1. J Biol Chem 2004;279:28122–31.
35. Lee AV, Weng CN, Jackson JG, Yee D. Activation of estrogen receptor-mediated gene transcription by IGF-I in human breast cancer cells. J Endocrinol 1997;152:39–47.
36. Straus DS, Pascual G, Li M, et al. 15-deoxy-$\Delta^{12,14}$-prostaglandin J_2 inhibits multiple steps in the NF-κB signaling pathway. Proc Natl Acad Sci U S A 2000;97:4844–9.
37. Oliva JL, Perez-Sala D, Castrillo A, et al. The cyclopentenone 15-deoxy-$\Delta^{12,14}$-prostaglandin J_2 binds to and activates H-Ras. Proc Natl Acad Sci U S A 2003;100:4772–7.
38. Liu XF, Bagchi MK. Recruitment of distinct chromatin-modifying complexes by tamoxifen-complexed estrogen receptor at natural target gene promoters *in vivo*. J Biol Chem 2004;279:15050–8.
39. Qin C, Burghardt R, Smith R, Wormke M, Stewart J, Safe S. Peroxisome proliferator-activated receptor γ agonists induce proteasome-dependent degradation of cyclin D1 and estrogen receptor α in MCF-7 breast cancer cells. Cancer Res 2003;63:958–64.
40. Valachovicova T, Slivova V, Bergman H, Shuherk J, Sliva D. Soy isoflavones suppress invasiveness of breast cancer cells by the inhibition of NF-κB/AP-1-dependent and -independent pathways. Int J Oncol 2004;25:1389–95.
41. Bell-Parikh LC, Ide T, Lawson JA, McNamara P, Reilly M, FitzGerald GA. Biosynthesis of 15-deoxy-$\Delta^{12,14}$-PGJ_2 and the ligation of PPARγ. J Clin Invest 2003;112:945–55.
42. Shibata T, Kondo M, Osawa T, Shibata N, Kobayashi M, Uchida K. 15-deoxy-$\Delta^{12,14}$-prostaglandin J_2. A prostaglandin D_2 metabolite generated during inflammatory processes. J Biol Chem 2002;277:10459–66.